On the tail of the overlap probability distribution in the Sherrington–Kirkpatrick model

2003 J. Phys. A: Math. Gen. 36 15

(http://iopscience.iop.org/0305-4470/36/1/302)

INSTITUTE OF PHYSICS PUBLISHING JOURNAL OF PHYSICS A: MATHEMATICAL AND GENERAL

J. Phys. A: Math. Gen. **36** (2003) 15–27 PII: S0305-4470(03)38523-3

On the tail of the overlap probability distribution in the Sherrington–Kirkpatrick model

Alain Billoire[1], **Silvio Franz**[2] **and Enzo Marinari**[3]

[1] Service de Physique Théorique, CEA/DSM/SPhT, Laboratoire associé au CNRS, CEA-Saclay, 91191 Gif-sur-Yvette Cédex, France
[2] ICTP, Strada Costiera 11, PO Box 563, 34100 Trieste, Italy
[3] Dipartimento di Fisica, SMC and UdR1 of INFM and INFN, Università di Roma *La Sapienza*, P A Moro 2, 00185 Roma, Italy

E-mail: billoir@spht.saclay.cea.fr, franz@ictp.trieste.it and enzo.marinari@roma1.infn.it

Received 17 June 2002, in final form 17 October 2002
Published 10 December 2002
Online at stacks.iop.org/JPhysA/36/15

Abstract

We investigate the large deviation behaviour of the overlap probability density in the Sherrington–Kirkpatrick (SK) model using the coupled replica scheme, and we compare with the results of a large-scale numerical simulation. In the spin glass phase we show that, generically, for any model with continuous replica symmetry breaking (RSB), $1/N \log P_N(q) \approx -\mathcal{A}(|q| - q_{EA})^3$, and we compute the first correction to the expansion of $\mathcal{A}$ in powers of $T_c - T$ for the SK model. We also study the paramagnetic phase, where results are obtained in the replica symmetric scheme that do not involve an expansion in powers of $q - q_{EA}$ or $T_c - T$. Finally we give precise semi-analytical estimates of $P(|q| = 1)$. The overall agreement between the various points of view is very satisfactory.

PACS numbers: 75.50.Lk, 75.10.Nr, 75.40.Gb

(Some figures in this article are in colour only in the electronic version)

1. Introduction

Although the solution of the Sherrington–Kirkpatrick (SK) model was proposed more than two decades ago [1], and its physical interpretation is (now) quite clear [2], some fundamental aspects of the model are still poorly understood, such as the problem of the timescales of the model [3], and the question of chaos with respect to temperature variations [4, 5], just to quote some recent works.

In this paper, we revisit the question of the large deviation behaviour of the order parameter probability distribution $P_N(q)$ of the SK model [6–8], using new analytical results, much improved numerical data and refinements in the data analysis.

In the usual mean field approximation, the probability distribution of the order parameter $P_N(m)$ is read from the free energy considered as a function of the order parameter. This method cannot be pursued in the replica approach, since the replica free energy has no physical interpretation for values of the order parameter different from the saddle point [2]. The coupled replica method was proposed in [6] to circumvent this problem and used in [7, 8]. In short, the replica method is applied to a system of two identical copies of the original system with a constrained value of the mutual overlap q, with the result

$$\frac{1}{N}\log P_N(|q| > q_{EA}) = -\mathcal{A}(|q| - q_{EA})^3 + \mathcal{O}((|q| - q_{EA})^4)$$

where q_{EA} is the Edwards–Anderson order parameter (the maximum allowed value for the overlap in the infinite volume limit). The proportionality coefficient $\mathcal{A}$ was computed in [6] to zeroth order in $\tau = \left(T_c^2 - T^2\right)/2T_c$. In order to obtain a value of the coefficient $\mathcal{A}$ to compare with the results of our large-scale simulation using the parallel tempering algorithm, we compute here the first-order term in τ. We also present semi-analytical results for $P(|q| = 1)$. For $T \geqslant T_c$ we present the results of an exact calculation, made in the replica symmetric scheme, that is limited neither to small q nor to the vicinity of T_c. This calculation corroborates well the other analytical and numerical results.

There are two aspects in the comparison made between the analytical results and the Monte Carlo data. The first is to (cross) check both results. This is important since, on the one hand, the analytical computation is very delicate and involves some unproven assumptions. The simulation is, on the other hand, limited to small systems, a finite number of disorder samples and finite statistics. Both approaches are very complementary. The second aspect is in checking how much of the infinite volume physics (at low temperatures, in the spin glass phase) is already encoded in the sizes we can effectively study on our current state-of-the-art computers (up to $N = 4096$ in the present case). We will see that, as far as the present computation is concerned, things do work well and we are moving in the right direction.

2. Large deviations in $P_N(q)$ for $|q| > q_{EA}$

In this section[4] we sketch the main steps and give the results of our computations of the function $P_N(q)$ in the large deviation regime, i.e. for $|q| > q_{EA}$, for both $T < T_c$ and $T \geqslant T_c$.

The overlap probability distribution $P_{N,J}(q)$ depends on the disorder sample J, and the function $P_N(q)$ is obtained as $\overline{P_{N,J}(q)}$, where the over-bar denotes the disorder average. It is well known that in the thermodynamic limit the disorder average of $P_{N,J}(q)$ is non-vanishing[5] in the interval $[0, q_{EA}]$, while sample-to-sample fluctuations remain strong even for large systems [2]. The probability of the complementary interval, i.e. of events with $q > q_{EA}$, is exponentially small in the system size [6]. For typical samples we have, independently of the disorder realization,

$$P_{N,J}(q) \approx \tilde{P}_N(q) \propto \exp(-\beta N F(q)) \tag{1}$$

where $\beta = 1/T$ and $F(q)$ is the self-averaging free energy cost of keeping two replicas at a mutual overlap q:

$$F(q) = -\frac{T}{N}\log\left(\frac{1}{Z^2}\sum_{\{\sigma_i,\tau_i\}} \mathrm{e}^{-\beta(H(\sigma)+H(\tau))}\left(q - \frac{1}{N}\sum_i \sigma_i\tau_i\right)\right). \tag{2}$$

[4] In the following we will take, without loss of generality, $q > 0$ (assuming, for example, the presence of a suitable infinitesimal magnetic field).

[5] We assume that our starting Hamiltonian is symmetric under global spin reversal.

It is quite natural to expect that, in the thermodynamic limit, $P(q) = \tilde{P}(q)$. In an alternative scenario, the fluctuations of $P_{N,J}(q)$ are dominated by rare (i.e. having exponentially vanishing probability) samples, causing $\overline{P_{N,J}(q)}$ to be different from $\tilde{P}_N(q)$. We will discuss this issue with our numerical simulations in the next section.

Let us start with the case $T < T_c$. In [6] the computation of $F(q)$ has been performed using the method of coupled replicas in the glassy phase ($T < T_c$) close to T_c, with the result that, in leading order in both $\tau \equiv \left(T_c^2 - T^2\right)/2T_c$ and $q - q_{EA}$, we have $F = 1/6(q - q_{EA})^3$. Let us now perform the computation of the pre-factor of the cubic term to the next order in τ. In order to compute $F(q)$ we have to replicate n times both the spins σ_i and the spins τ_i. Two order parameter matrices appear:

$$Q_{ab} = \langle \sigma_a \sigma_b \rangle = \langle \tau_a \tau_b \rangle \qquad \text{and} \qquad P_{ab} = \langle \sigma_a \tau_b \rangle \qquad a, b = 1, \ldots, n. \tag{3}$$

We make a Parisi ansatz [2] for both Q and P, introducing two functions $q(x)$ and $p(x)$. We now recast the two $n \times n$ matrices into a single $2n \times 2n$ bold-faced matrix

$$\mathbf{Q} = \begin{pmatrix} Q & P \\ P & Q \end{pmatrix}. \tag{4}$$

Let us consider in all generality any system that is described in the uncoupled case by the free energy functional $F[Q]$ in terms of the usual replica matrix. The same system when coupled according to equation (2) has a free energy functional of the form

$$F_2[Q, P] = F[\mathbf{Q}] + \epsilon \left(nq - \sum_{a=1}^{n} P_{aa} \right) \tag{5}$$

where ϵ is a Lagrange multiplier associated with the δ-function in equation (2).

If the problem of a single, uncoupled, system admits a continuous solution $q_F(x)$ (that we suppose is known), it can be shown that the corresponding variational equations related to the coupled problem admit two simple solutions [9].

A first solution has $\Delta F = \epsilon = 0$, with functions $q(x)$ and $p(x)$ that can be constructed explicitly from $q_F(x)$

$$q(x) = \begin{cases} q_F(2x) & 0 \leqslant x \leqslant \frac{\tilde{x}}{2} \\ q & \frac{\tilde{x}}{2} \leqslant x < \tilde{x} \\ q_F(x) & 1 \geqslant x \geqslant \tilde{x} \end{cases} \qquad p(x) = \begin{cases} q_F(x) & 0 \leqslant x \leqslant \tilde{x} \\ q & \tilde{x} \leqslant x < 1 \end{cases} \tag{6}$$

where the point $\tilde{x}$ is defined by the equation $q_F(\tilde{x}) = q$.

In the second solution $q(x) = p(x)$. This second solution becomes degenerate with the first solution at $q = q_{EA}$. If we use the usual replica approach to maximize the free energy with respect to the Q-parameters (in agreement with the physical intuition about the problem) we will select the first solution in the region with $q < q_{EA}$ and the second in the region with $q > q_{EA}$, where it has a larger free energy.

Note that, while the first solution has a flat free energy $F(q) = 0$, the second, as a consequence of the facts that

- it coincides with the first solution for $q = q_{EA}$, and
- it has to be a solution of the saddle-point equations,

must be such that $\frac{\mathrm{d}F(q)}{\mathrm{d}q}\big|_{q=q_{EA}} = 0$. All these properties together imply that generically $F(q) = \mathcal{A}(q - q_{EA})^3$, where $\mathcal{A}$ is a problem- and temperature-dependent constant. Of course, the accidental vanishing of $\mathcal{A}$ is an allowed possibility, and in this case $F(q)$ would be of order five or higher.

Let us now turn to the explicit computation for the SK model close to T_c. In this case the replica free energy density can be written as

$$F_2[Q, P] = \tau \operatorname{Tr} \mathbf{Q}^{*2} + \frac{1}{3} \operatorname{Tr} \mathbf{Q}^{*3} + \frac{1}{4} y \sum_{\alpha,\beta}^{1,2n} \mathbf{Q}^{*4}_{\alpha,\beta} + \epsilon \left(nq - \sum_{a=1}^{n} P^*_{aa} \right) \tag{7}$$

where $y = 2/3$, but it will be kept as a parameter during the computation. We have defined $Q^*_{ab} \equiv Q_{ab}/T^2 \simeq Q_{ab}(1 + 2\tau)$ and $P^*_{ab} \equiv P_{ab}/T^2$. Here the solution can be found explicitly, and writing $\tilde{P}^* = P^*_{aa}$ and inserting $P^*_{ab} = Q^*_{ab}$ $(a \neq b)$ in the equation of motion we find that the matrix Q^* verifies the following equation

$$(\tau + \tilde{P}^*) Q^*_{ab} + (Q^{*2})_{ab} + \frac{y}{2} Q^{*3}_{ab} = 0 \tag{8}$$

which is identical to the solution of the free problem with $\tau \to (\tau + \tilde{p}^*)/2$ and $y \to y/2$. Then, plugging the known solution of the free problem into the free energy functional it is easy to derive the result:

$$F(q) = \left(\tfrac{1}{6} - \tfrac{3}{4} \tau y \right) (q^* - q^*_{EA})^3. \tag{9}$$

Or, using the original definition of q, and setting $y = 2/3$,

$$F(q) = \left(\tfrac{1}{6} + \tfrac{1}{2} \tau \right) (q - q_{EA})^3. \tag{10}$$

Let us now discuss the paramagnetic phase, where $T > T_c$. Here $q_{EA} = 0$ and we have to select the solution that always has $p(x) = q(x)$ for $q \geqslant 0$ and $p(x) = -q(x)$ for $q < 0$. Let us consider the replica symmetric free energy, corresponding to $\tilde{P} = q$, $q(x) = \operatorname{sgn}(q)$, $p(x) = q_0$. For simplicity we will write, as before, equations valid for $q > 0$, keeping in mind that the free energy $F(q)$ has to satisfy $F(-q) = F(q)$.

Defining $Dy = \mathrm{e}^{-\frac{1}{2}y^2} \big/ \sqrt{2\pi}\, \mathrm{d}y$, standard manipulations lead to the expression

$$\begin{aligned} F(q) = -\frac{\beta}{2} \left(1 + q^2 + 2q_0^2 - 2q_0 - 2q q_0 \right) - T \log 2 + T \nu q \\ - T \int Dy \log[\mathrm{e}^{-\nu} + \mathrm{e}^{\nu} \cosh(2\beta \sqrt{q_0} y)] \end{aligned} \tag{11}$$

which has to be extremized with respect to q_0 and ν (the Lagrange multiplier associated with q). This leads to the saddle-point equations

$$q = \int Dy \frac{-\mathrm{e}^{-\nu} + \mathrm{e}^{\nu} \cosh(2\beta \sqrt{q_0} y)}{\mathrm{e}^{-\nu} + \mathrm{e}^{\nu} \cosh(2\beta \sqrt{q_0} y)} \tag{12}$$

$$q_0 = \frac{1 + q}{2} - \frac{1}{2\beta \sqrt{q_0} y} \int Dy \frac{y\, \mathrm{e}^{\nu} \sinh(2\beta \sqrt{q_0} y)}{\mathrm{e}^{-\nu} + \mathrm{e}^{\nu} \cosh(2\beta \sqrt{q_0} y)}. \tag{13}$$

These equations always have the trivial solution $q_0 = 0$, $\nu = \tanh^{-1} q$, which is correct at high enough temperatures and small values of q. A small q_0 expansion reveals that a solution with $q_0 \neq 0$ is possible for $q \geqslant T - 1 = q_c(T)$. Notice that

- for $T \leqslant 1$ the solution is non-trivial for all values of q;
- for $T > 2$ the solution is always $q_0 = 0$;
- for $1 < T \leqslant 2$ there is a phase transition from the solution $q_0 = 0$ for $q < T - 1$ to a solution $q_0 \neq 0$ for $q > T - 1$.

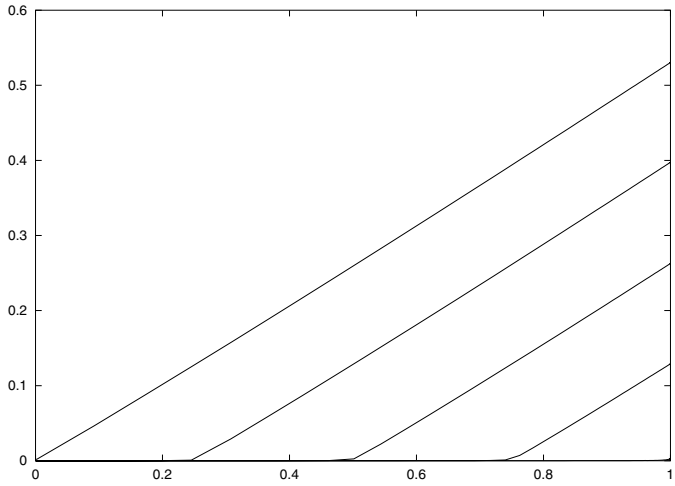

Figure 1. The induced overlap q_0 as a function of the mutual overlap q that we force on the system for $T = 1.0$, 1.25, 1.5, 1.75 and 2.00 (from right to left, with $q_0 = 0\ \forall q$ for $T = 1$).

The correct solution in this last domain should break the replica symmetry. Close to $q_c(T)$ a small q expansion, as in the previous section, can be used even for large values of $T_c - T$. For $q_c(T) - q \approx 1$ we only consider the replica symmetric approximation. It is clear that if we impose $q = 1$ the system behaves as a single system with temperature $T/2$, and we understand therefore why $q_c(2) = 1$.

The $q_0 = 0$ solution gives a free energy

$$F(q) = -\frac{\beta}{2}(1 + q^2) - 2T \log 2 + T\nu q - T \log(\cosh(\nu)). \tag{14}$$

In figure 1 we show the solution for q_0 as a function of q. For $q = 1$ we find that q_0 takes, as it should, the value $q_{RS}(T/2)$, i.e. the Edwards–Anderson value at temperature $T/2$ in the replica symmetric (RS) approximation. The functional form of q_0 is well approximated for all values of T by $q_0(q) = q_{RS}(T/2)(q - q_c(T))$, although small quadratic deviations from this form can be observed. In figure 2 we also plot the related free energy.

3. Numerical versus analytical results

In the following we use our numerical results obtained from simulations of the $J_{i,j} = \pm 1$ SK model toward two different goals, that we have already partially discussed in the introduction. First, we want to carry out a numerical check of our analytical findings; it is clear that we are dealing with a complex set of equations, we are working in some asymptotic regimes, and this implies that a numerical check is quite welcome. The second issue is perhaps less direct but also very crucial. It is important to understand how well numerical simulations performed on a finite lattice encompass the infinite volume physics, and, at the same time, how good a control we can have on the temperature range that we explore. The issue of the infinite volume limit is indeed of very great importance, and it is crucial to verify that exotic phenomena (such as the large deviation regime we are discussing here) are already well quantified in the region of lengths we can study with present-day computer facilities.

Our large-scale numerical simulations are based on the numerical optimized Monte Carlo technique of parallel tempering [10]. These have already been used in our recent paper on the problem of chaos [5] (but for the addition of the data obtained on a $N = 128$ site lattice).

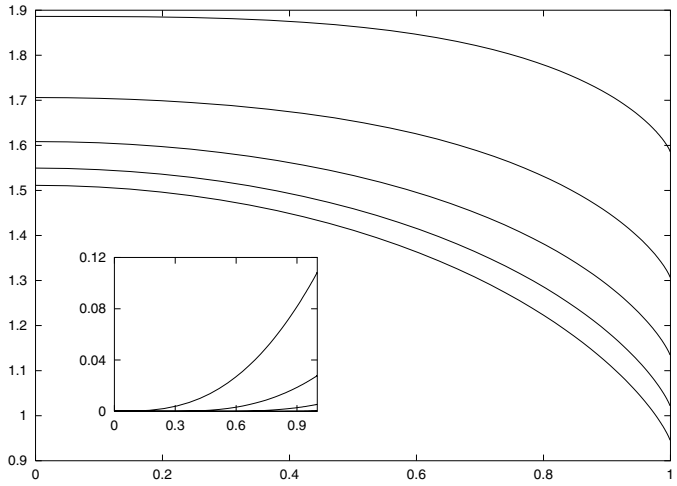

Figure 2. The free energy $-\beta F(q)$ for the same values of the temperature as in figure 1 (from top to bottom). In the inset we plot, for the same set of temperatures again, the difference $-\beta(F_0(q) - F(q))$, where $F_0(q)$ is computed with the trivial solution $q_0 = 0$ (from top to bottom). The difference is zero for $T = 2$ and very small for $T = 1.75$.

We have analysed 1024 different disorder realizations for $N = 64$, 256 and 1024 sites, 256 for $N = 4096$ and 8192 for $N = 128$. We go down to a minimal temperature value $T_m = 0.4\,T_c = 0.4$, and we use 0.4×10^6 iterations for thermalizing and 10^6 iterations for measurements. We normalize probability distributions according to $\int_{-1}^{1} P_N(q)\,\mathrm{d}q = 1$.

The first question we discuss is whether it is appropriate to measure the quenched average

$$\beta\tilde{F}(q) = N^{-1}\,\overline{\log P_{N,J}(q)} \tag{15}$$

(i.e. the quantity computed using the two-replica method) or if it is better to measure the annealed average

$$\beta F(q) = N^{-1}\log\overline{P_{N,J}(q)} \tag{16}$$

(a quantity that is much easier to measure with the Monte Carlo simulation). In section 2 we have discussed the issue, arguing that these two averages could differ because of rare samples. We now use our numerical data to answer this question.

In figure 3 we show results for both the quenched (equation (15)) and the annealed (equation (16)) averages at $T = 0.4$ as a function of q. We plot data for $N = 64, 128, 256$ and 1024. In order to make the figure readable:

1. we have subtracted from the different measurements a term $1/3\log N$, that separates the points from different system sizes;
2. we have not drawn the $F(q)$ data as points with statistical error bars, but we have drawn a line through the data points.

The (few) data points for $\tilde{F}(q)$ are drawn with statistical error bars (estimated from the variance of sample-to-sample fluctuations). It appears that the data for $\tilde{F}(q)$ are confined to a much smaller q range than the data for $F(q)$. This is expected since, for a given value of q, $\tilde{F}(q)$ is well defined only if (the estimate of) $P_N(q)$ is larger than zero for every sample, whereas $F(q)$ is well defined as soon as the average $P_N(q)$ is larger than zero.

Figure 3 shows that for large system sizes the annealed and quenched estimates are consistent. The same conclusion holds for all other temperature values that we have considered.

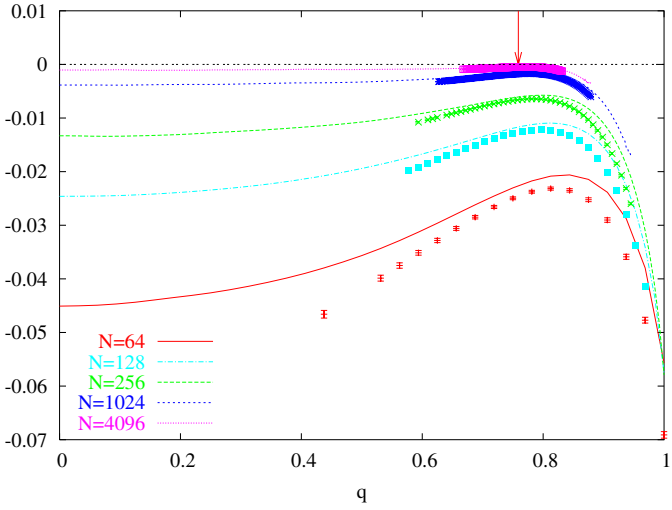

Figure 3. $1/N \log(P_N(q)N^{-\frac{1}{3}})$ versus q for $T = 0.4$: annealed ($F(q)$, represented by lines) and quenched ($\tilde{F}(q)$, represented by points with error bars) estimates. The vertical arrow indicates the value of q_{EA} at $T = 0.4$.

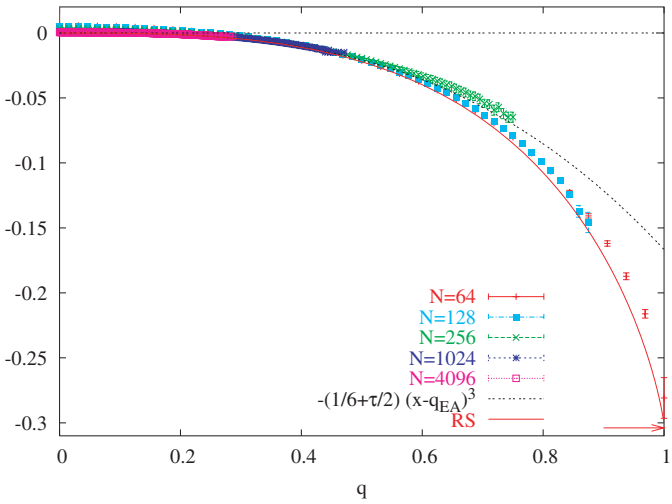

Figure 4. $1/N \log P_N(q)$ versus q for $T = 1$. The points with error bars are numerical data from different lattice sizes, and the dotted line is from the perturbative estimate in the spin glass phase. A horizontal arrow indicates the exact $q = 1$ value. The full line (labelled 'RS') is from equation (11).

Because of this, in what follows we only consider the annealed averages $P_N(q)$ and $F(q)$. We estimate statistical errors on our observables using a jack-knife procedure [11].

Our second (and main) numerical goal is to verify the predictions of equation (10) that predict asymptotically a cubic behaviour of $1/N \log P_N(q)$ in $q - q_{EA}$, with a coefficient computed at order τ. Now, is all that correct? Can we already observe this behaviour on the lattice size that we are able to thermalize in the spin glass phase?

We report on our results at different values of the temperature ($T = 1.0, 0.8, 0.6$ and 0.4) in figures 4, 5, 6 and 7, respectively. We plot the theoretical prediction of equation (10) by

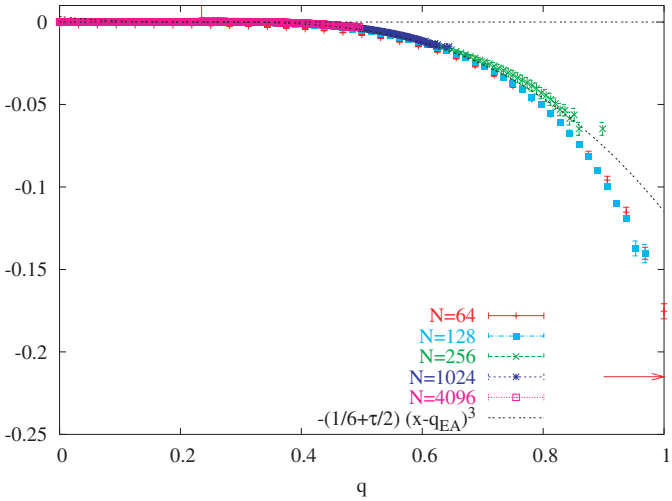

Figure 5. As in figure 4 but with $T = 0.8$. The additional vertical arrow indicates the value of q_{EA}.

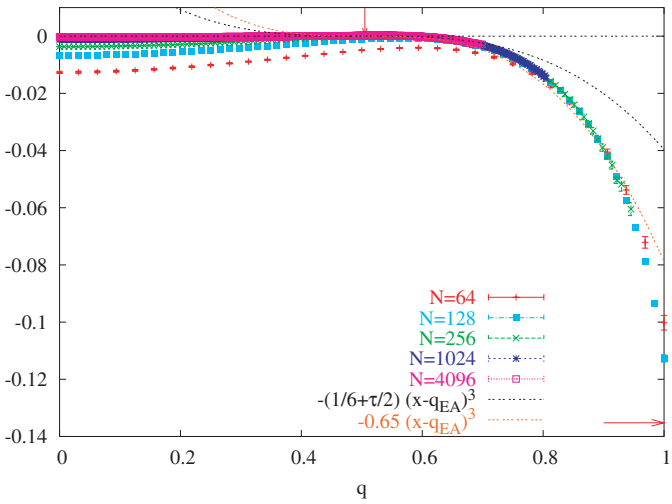

Figure 6. As in figure 5 but with $T = 0.6$. The additional lower dotted curve is drawn using a coefficient modified by hand, accounting for the renormalization of the temperature when τ increases.

the dotted line, and we give the analytic value of $P_N(q = 1)$ by a horizontal arrow (see the discussion later).

All figures show that results for the systems of different sizes converge to a common (N-independent) function; our results for the excess free energy are indeed in the asymptotic regime. The careful reader will notice, however, that only the limit $\lim_{\to\infty} 1/N \log P_N(q)$ is predicted. There is accordingly an order $1/N$ ambiguity in the vertical offsets of our plots for $1/N \log P_N(q)$. Plotting, for example, $1/N \log(P_N(q)N^{-1/3})$ would result in figures which would look slightly different.

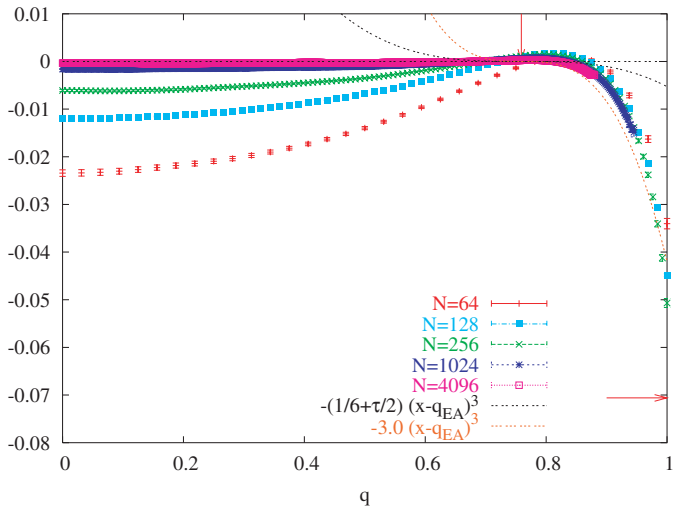

Figure 7. As in figure 6 but with $T = 0.4$.

At $T = 1$, where $q_{EA} = 0$, the agreement of our data with the theoretical prediction is very good at least up to $q = 0.6$. Also at $T = 0.8$, where q_{EA} is slightly larger than 0.2 (i.e. still very small) the agreement is very good in a very large q range (up to $q \simeq 0.8$). In all these analyses, we have used the value of q_{EA} computed by Crisanti and Rizzo by numerical integration [12] of the Parisi solution of the SK model (e.g. we are not using q_{EA} computed to order τ).

At $T = 0.6$, where q_{EA} is of order 0.5 and a small τ expansion with two terms starts to be inappropriate, the agreement becomes less good. To take into account the fact that here τ is large and there is an effective renormalization (when $T = 0.6$ the first-order correction in equation (10) is equal to 0.16 while the leading term is equal to $1/6$), we have added a further curve where we substitute the pre-factor we have computed analytically in equation (10) with some effective value, that optimizes the matching of the analytical form to the numerical data; this very much improves the agreement. This effect is even more dramatic at $T = 0.4$, where again a cubic dependence with a renormalized pre-factor fits the data very well in a large $q > q_{EA}$ range.

Our third numerical goal concerns the value of $P_N(q)$ at $q = 1$ (that we plot with a horizontal arrow in the four figures). We use the simple relation

$$\frac{1}{N} \log P_N(q = 1) = -\frac{2}{T}\left(\mathcal{F}_{\frac{T}{2}} - \mathcal{F}_T\right) \tag{17}$$

between $P_N(q = 1)$ at temperature T and the free energy of the SK model at temperatures T and $T/2$. We take for $\mathcal{F}_T$ the infinite volume free energy of the model derived with high precision in [12] from the Parisi solution.

We see from figures 4–7 that the prediction of equation (17) for $P_N(q = 1)$ is smaller than the value which formula (10) takes at $q = 1$. Obviously, this is expected, since equation (10) is the first term in an expansion in powers of $q - q_{EA}$, and is not supposed to be valid up to the $q = 1$ boundary, where higher orders cannot be neglected (the function is presumably singular at $q = 1$). Note, however, that the interplay between finite size effects and higher orders in $T_c - T$ is not trivial. It can be studied numerically using the multi-overlap algorithm [13] which allows us to measure $P_N(q)$ with high accuracy up to $q = 1$. However, parallel tempering numerical data, when pushed to very high statistics, confirm already in a remarkable

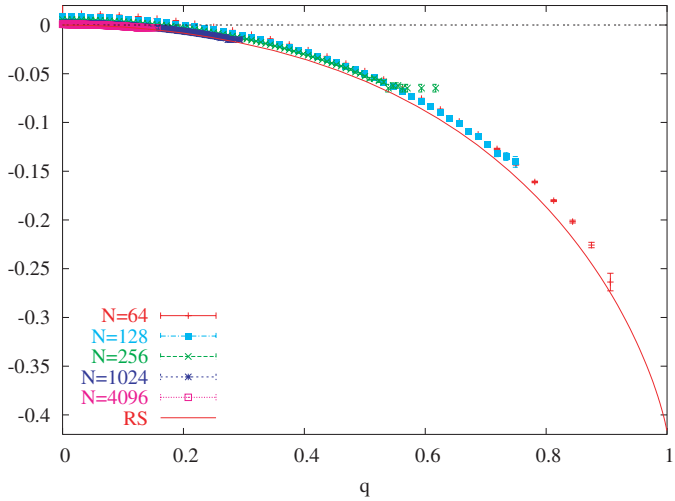

Figure 8. As in figure 6 but with $T = 1.3$.

way the analytical value (this can only be done for small lattice sizes). At $T = 1$ we are able to push the $N = 64$ lattice up to $q = 1$ and to keep under control the limit of the $N = 128$ lattice. At lower T values, the check is slightly more difficult, but we see that the $q = 1$ limit of larger and larger lattices approaches the analytic value better and better.

It can be shown that the situation is well under control for $T \geqslant 1$ by comparing the numerical data, in the whole $q \in [0, 1]$ range, with the results of our RS computation of equation (11). This is done in figures 4 for $T = 1.0$ and 8 for $T = 1.3$ (the highest temperature, alas, in our parallel tempering simulation). The first figure shows the full line (labelled 'RS') cleanly overshooting the dotted line, to reach the $q = 1$ axis slightly above (as expected) the exact $q = 1$ limit[6]. Also, figure 8 shows again the agreement of our numerical data with the replica calculation.

Equation (10) suggests [7, 8] that (for $T < T_c$) $P_N(q)$ scales asymptotically as

$$P_N(q)N^{-\frac{1}{3}} = \mathcal{F}(N(q - q_{EA})^3) \qquad \text{for} \quad q > q_{EA} \tag{18}$$

with $\mathcal{F}(z) \propto \exp(-Az)$, with some positive constant A, for large z. If the above formula holds, down to the maximum of $P_N(q)$, this implies that the location of the peak of the probability distribution of the overlap on a lattice of size N, which we denote by $q_{\max}(N)$, has to behave like

$$q_{\max}(N) = q_{EA} + cN^{-\frac{1}{3}}$$

a behaviour that has indeed been verified with high accuracy in a previous work [5].

In what follows we accordingly look for a scaling law in the form

$$P_N(q)N^{-\frac{1}{3}} = \mathcal{G}(N(q - q_{\max(N)})^3) \tag{19}$$

using the numerical estimates obtained for $q_{\max(N)}$. Figures 9, 10, 11 and 12 are scaling plots of $\log(P_N(q)N^{-1/3})$ versus $N(q - q_{\max}(N))^3$. The figures clearly exhibit the predicted cubic limiting behaviour. At $T = T_c$ the data are, furthermore, in excellent agreement with the predicted slope. At $T = 0.8$ the term linear in τ computed in this paper is essential in order to obtain good agreement with the data. $T = 0.6$ and $T = 0.4$ are clearly too far from T_c to

[6] This strongly indicates that the correct large q behaviour in figures 4 and 5 is given by the $N = 64$ and 128 data, and that the rightmost $N = 256$ points are somewhat misleading

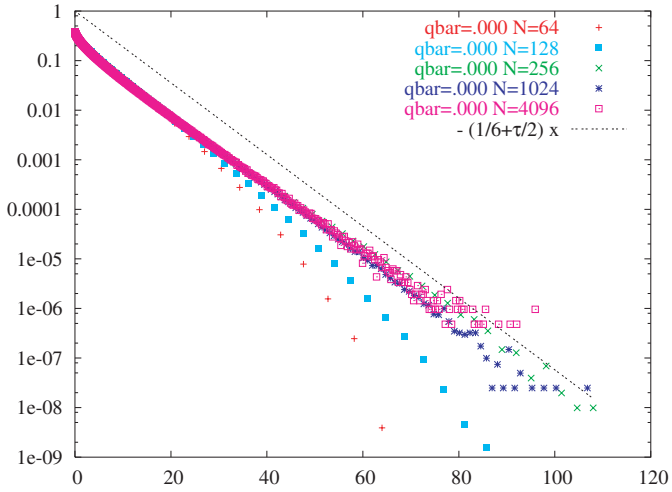

Figure 9. Scaling plot of $P_N(q)N^{-\frac{1}{3}}$ as a function of $(q - q_{\max}(N))^3 N$ for $T = 1.0$, compared with the coupled replica estimate (with arbitrary normalization). Our estimate of $q_{\max}(N)$ is reported in the figure labelled as **qbar** (it is obviously zero at T_c).

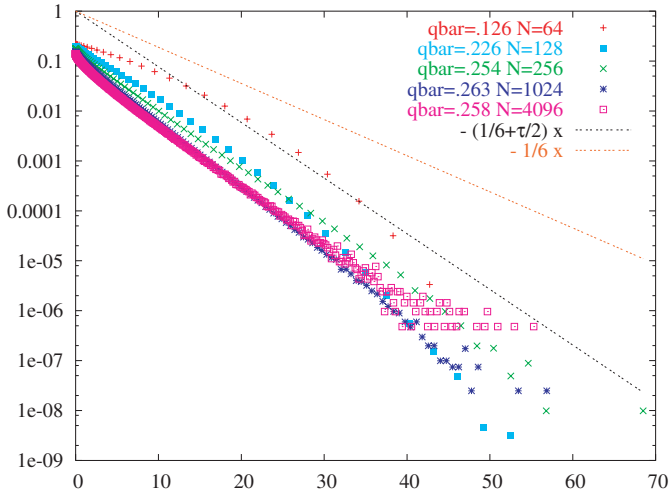

Figure 10. As in figure 9 but for $T = 0.8$. The coupled replica estimate is plotted with and without the term linear in τ. Note that $q_{\max}(N)$ is not well determined on small systems at this temperature, i.e. close to T_c.

obtain a good result for the slope with only two terms in the expansion in powers of τ. Scaling is violated on small systems for the rightmost points. This must be so since these are points with q close to one, and we have seen before that close to one the behaviour is not cubic.

It should be stressed that with our data scaling in $(q - q_{\max}(N))^3 N$ (equation (18)) is much better than scaling in $(q - q_{EA})^3 N$ (equation (19), using the very precise data for q_{EA} by Crisanti and Rizzo). One reason for this better agreement may be that for $q > q_{EA}$ the inflection point of $(q - q_{\max(N)})^3 N$ mimics the maximum of $1/N \log P_N(q)$. Scaling plots as a function of $(q - q_{EA})^3 N$ with an *ad hoc* effective N-independent q_{EA} appear (in a small z interval) in [7] for $T = 0.8$, and in [8] for $T = 0.5$.

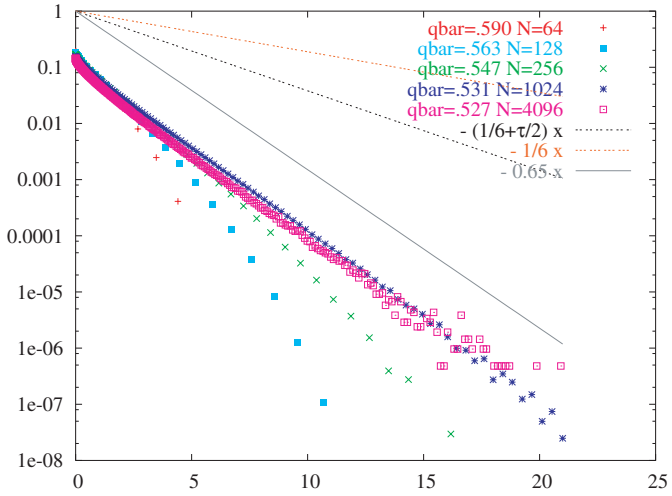

Figure 11. As in figure 10 but for $T = 0.6$. The additional dotted line is drawn using the same hand-modified coefficient as in figure 6.

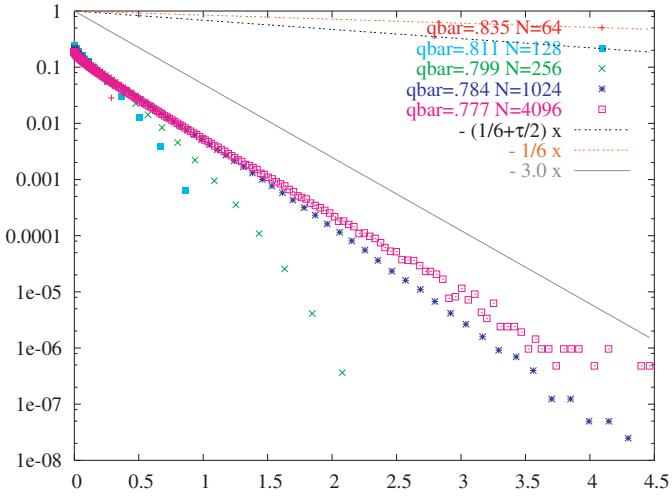

Figure 12. As in figure 9 but for $T = 0.4$. The additional dotted line is drawn using the same hand-modified coefficient as in figure 7.

4. Conclusions

The results of these analyses are very positive. We have first argued that the large deviation leading behaviour of $P_N(q > q_{EA})$ is generically $1/N \log P_N(q) = -\mathcal{A}\,(q - q_{EA})^3$, and we have computed the first corrections to the expansion of $\mathcal{A}$ in powers of $T_c - T$ for the SK model.

Data from numerical simulations confirm that this behaviour can be already detected for moderate lattice sizes. Firstly, we have seen that we can easily take an annealed average of F. Secondly we have analysed the details of the cubic behaviour, and checked the validity of the perturbative estimate of the pre-factor; close to T_c it works very well, while far away from T_c

a simple renormalization improves the agreement substantially. Our very accurate data have allowed a detailed analysis of the $P(q = 1)$ value, again allowing for a positive check of the analytical result. For $T \geqslant T_c$ an exact computation in the replica symmetric scheme shows well the crossover from the $q \approx q_{EA}$ behaviour to the ultimate limit $q = 1$. Finally, we have shown that the scaling plots for $P_N(q)$ improve appreciably if we use $(q - q_{\max}(N))^3 N$ as the scaling variable, showing clearly the predicted cubic behaviour of $\log(P_N(q)N^{-1/3})$.

Acknowledgments

We thank A Crisanti and T Rizzo for providing us with their unpublished numerical evaluations of quantities in the SK model, and we also thank Giorgio Parisi for discussions. SF thanks the SPhT Saclay for a visiting professor fellowship and for warm hospitality in the months of October to December 2001, during which part of this work was performed.

References

[1] Parisi G 1979 *Phys. Rev. Lett.* **43** 1754
[2] Mézard M, Parisi G and Virasoro M A 1987 *Spin Glass Theory and Beyond* (Singapore: World Scientific)
[3] MacKenzie N D and Young P 1982 *Phys. Rev. Lett.* **49** 301
Billoire A and Marinari E 2001 *J. Phys. A: Math. Gen.* **34** L1
[4] See, for example, Billoire A and Marinari E 2000 *J. Phys. A: Math. Gen.* **33** L265 and references therein
[5] Billoire A and Marinari E 2002 *Preprint* cond-mat/0202473 (*Europhys. Lett.* at press)
[6] Franz S, Parisi G and Virasoro M A 1992 *J. Physique* I **2** 1869
[7] Parisi G, Ritort F and Slanina F 1993 *J. Phys. A: Math. Gen.* **26** 3775
[8] Ciria J C, Parisi G and Ritort F 1993 *J. Phys. A: Math. Gen.* **26** 6731
[9] Franz S *PhD Thesis* unpublished
[10] For an introduction see, for example, Marinari E 1998 *Advances in Computer Simulations* ed J Kerstez and I Kondor (Berlin: Springer) p 50 (*Preprint* cond-mat/9612010)
[11] Flyvbjerg H 1998 *Advances in Computer Simulations* ed J Kerstez and I Kondor (Berlin: Springer)
[12] Crisanti A and Rizzo T 2002 *Phys. Rev.* E **65** 046137 (*Preprint* cond-mat/0111037) and private communication
[13] Berg B, Billoire A and Janke W 2002 *Phys. Rev.* E **65** 045102R (*Preprint* cond-mat/0108034)
Berg B, Billoire A and Janke W 2002 *Preprint* cond-mat/0205377 (*Phys. Rev.* E. at press)